Biochemical and Biophysical Research Communications 394 (2010) 211–216

Contents lists available at ScienceDirect

Biochemical and Biophysical Research Communications

journal homepage: www.elsevier.com/locate/ybbrc

SMN and the Gemin proteins form sub-complexes that localise to both stationary and dynamic neurite granules

Adrian G. Todd [a], Debra J. Shaw [a], Robert Morse [a], Howard Stebbings [b], Philip J. Young [a,*]

[a] Functional Neurobiology, Institute of Biomedical and Clinical Science, Peninsula Medical School, St Luke's Campus, Exeter, UK
[b] School of Biosciences, University of Exeter, Streatham Campus, Exeter, UK

ARTICLE INFO

Article history:
Received 16 February 2010
Available online 25 February 2010

Keywords:
Neurite transport
SMN
Gemin
Granules

ABSTRACT

Childhood spinal muscular atrophy (SMA) is caused by a reduction in survival motor neuron (SMN) protein. SMN is expressed in every cell type, but it is predominantly the lower motor neurones of the spinal cord that degenerate in SMA. SMN has been linked to the axonal transport of β-actin mRNA, a breakdown in which could trigger disease onset. It is known that SMN is present in transport ribonucleoproteins (RNPs) granules that also contain Gemin2 and Gemin3. To further characterise these granules we have performed live cell imaging of GFP-tagged SMN, GFP-Gemin2, GFP-Gemin3, GFP-Gemin6 and GFP-Gemin7. In all, we have made two important observations: (1) SMN granules appear metamorphic; and (2) the SMN–Gemin complex(es) appears to localise to two distinct subsets of bodies in neurites; stationary bodies and smaller dynamic bodies. This study provides an insight into the neuronal function of the SMN complex.

1. Introduction

Childhood spinal muscular atrophy (SMA) is an autosomal recessive disorder characterised by loss of the alpha-motor neurones of the spinal cord [1]. SMA has been divided into three clinical subgroups based on age of onset and clinical severity: types I, II and III, with type I being the most severe [1]. All three forms are caused by mutations of the survival motor neuron (*SMN*) gene [1,2]. There are two copies of the *SMN* gene; *SMN1*, deletions in which cause SMA; and *SMN2*, which is a disease-modifying gene [2,3].

Although SMN is a ubiquitously expressed protein, reductions in SMN protein levels trigger the targeted loss of the alpha-motor neurones. This specificity has still to be accounted for. However, emerging evidence suggests that the SMN protein is functionally implicated in the subcellular targeting of β-actin mRNA along neuronal axons [4–7]. Active transport of β-actin mRNA along axons from the cell body to the growth cones enables localised, 'on-demand' translation into β-actin protein [4]. This allows the levels of β-actin protein and production of actin-based filapodia at the neurite termini to be closely regulated, which permits maintenance of the dynamic interface at the neuromuscular junction [8]. Interestingly, *in vitro* cultures of SMA sensory- and motor-neurones demonstrate that motor neurones exhibit increased temporal demands of actin monomer turnover compared to their sensory counterparts [9]. If subcellular targeting of cytoskeletal precursors to peripheral regions of migrating cells to maintain actin dynamics is, at least partially SMN-dependent, a breakdown in this process arising from reduced amounts of SMN may provide a plausible explanation for selective motor neuronal vulnerability.

A variety of cellular components are actively transported in axons in transport granules (TGs). SMN forms sub-complexes within axons that can be classified into two categories: (1) larger granules that exhibit small/oscillatory movements; and (2) granules that exhibit bi-directional movement at speeds of up to 1 μm/s [4]. SMN granules within axons, regardless of their subtype (stationary or actively transported) have only been partially characterised. It is known that as well as SMN and ribosomal RNA [4], SMN granules in axons also contain ZBP1 [10–13], Gemin2 [5], Gemin3 [5] and hnRNPQ/R [14]. In addition, Gemin6 and Gemin7 have been shown to co-localise diffusely with SMN throughout the cytoplasm of PC12 cells [15]. It remains unclear whether: (1) the entire Gemin complex is involved specifically in the transport of β-actin mRNA; or (2) if the entire complex is present in stationary and/or actively transported SMN granules.

Here, we present data tracking the movement of GFP-tagged Gemin proteins in a human neuroblastoma cell line (SH-SY5Y). Firstly, we show that GFP-tagged SMN complex members (SMN, Gemin2, Gemin3, Gemin6 and Gemin7) are all efficiently targeted to transport granules in the neurites of differentiated SH-SY5Y cells. We then show that like SMN and Gemin2, Gemins 3, 6 and

* Corresponding author. Address: Clinical Neurobiology, Institute of Biomedical and Clinical Science, Peninsula Medical School, Heavitree Rd, Exeter EX1 2LU, UK. Fax: +44 1392 262926.
E-mail address: philip.young@pms.ac.uk (P.J. Young).

0006-291X/$ - see front matter © 2010 Elsevier Inc. All rights reserved.
doi:10.1016/j.bbrc.2010.02.158

7 form two subsets of neurite granules: (1) stationary granules, which are >5 μm in length; and (2) smaller transport granules, that move in a bi-directional manner at speeds averaging 0.38 μm/s. This analysis strengthens our understanding of the cellular dynamics of the SMN protein, and demonstrates that it forms complexes that are both dynamic and metamorphic.

2. Materials and methods

2.1. cDNA constructs

SMN was cloned into pEGFP as previously described [16]. Gemins were cloned into pEGFPc vectors (Clonetech™, BD Biosciences). Gemin2 was cloned into pEGFPc2 using primers Forward GATCGAA TTCATGCG CCGAGCGGAACTGGCTGGTTT, Reverse GATCGGATCCT CAAGATGGCTCA TCAGCTAAATCAC. The remaining Gemins were cloned into pEGFPc3 vectors using Gemin3 Forward GATCCTCGA GATGGCGGCGGCATTTGAAGCCTCGGG, Gemin3 Reverse GATCCTG CAGTCACTGGTTACTATGCATCATTTCTT; Gemin6 Forward GATCCTC GAGATGAGTGAATGGATGAAGAAAGGCCC, Gemin6 Reverse GATCA AGCTTTCATTGGGAAGCTGTAAGATGTCCTTC; Gemin7 Forward GA TCCTCGAGATGCAAACTCCAGTGAACATTCCCGT, Gemin7 Reverse GATCAAGCTTTTATGGCTTGAAGGTATATGAAATAA.

2.2. PCR conditions

Template cDNAs were amplified from carrier vectors pET (Gemin2), pCR2.1 (Gemin3), pEGFP (Gemin6), pEGFP (Gemin7) using *Pfu* polymerase and 35 cycles of 92 °C 45 s denature, 52 °C 45 s anneal, 68 °C 4 m 30 s extension. Post PCR, 10 μl of amplified product and 2 μl DNA loading dye were loaded on a 1% w/v agarose-TBE gel to ensure the correct size fragment had been amplified. Prior to ligation into pEGFP vectors, amplified PCR products were purified using QIAquick PCR purification kits (Qiagen). The use of betaine (Sigma–Aldrich) at a concentration of 300 mM was required for amplification of Gemin3. Once amplified each cDNA was digested and ligated into the pEGFP vector, as described elsewhere [16].

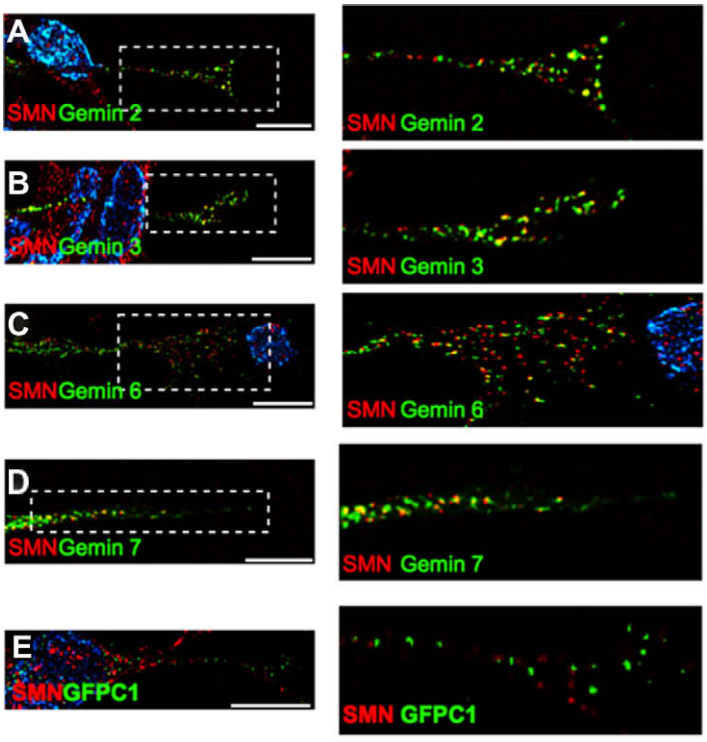

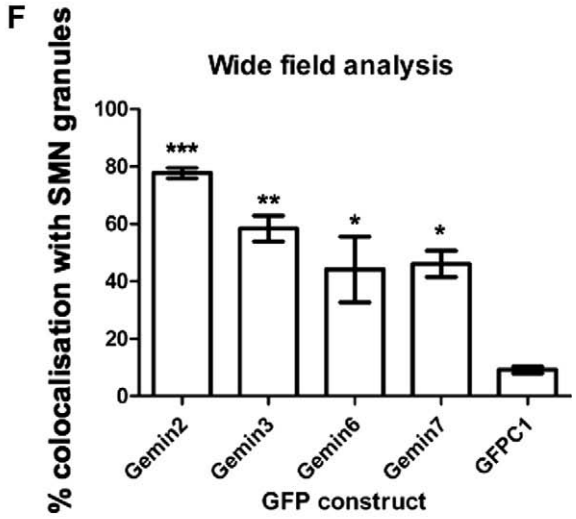

G

	Mean % co-localised with SMN in granules	Standard error of the mean (SEM)	Number of granules counted (n)
GFP-Gemin2	77.7	1.8	71
GFP-Gemin3	58.4	4.5	90
GFP-Gemin6	44.2	11.5	117
GFP-Gemin7	46.1	4.5	73
GFP-C1	9.2	1.7	91

Fig. 1. GFP-Gemins co-localise with endogenous SMN neurite granules. SH-SY5Y cells (1.25×10^5) transfected with 2 μg GFP-Gemin cDNA were plated at a density of 1×10^4 cells/ml in fetal calf (bovine) serum and retinoic acid (10 μM) supplemented DMEM and differentiated for 48 h. Cells expressing (A) GFP-Gemin2; (B) GFP-Gemin3; (C) GFP-Gemin6; (D) GFP-Gemin7; and (E) GFP-alone were counterstained with SMN using a monoclonal antibody (MANSMA1; [17]). Amplified images of specific regions are alongside original micrographs. The scale bars represent 20 μm. (F) Experiments were repeated in triplicate and the average number of GFP-positive neurite granules that also contain the endogenous SMN was recorded. The standard error of the mean (SEM; S_m) for each value is shown (error bars). Statistical analysis showed that collectively, GFP-Gemins are significantly more associated with SMN neurite granules than GFP-alone ($p < 0.05$).

2.3. Cell culture

SH-SY5Y cells were grown in RPMI-1640 (Invitrogen) supplemented with 10% Fetal Bovine Serum (Lonza), and 1% Penicillin and Streptomycin (Invitrogen).

2.4. Transient expression studies

For endogenous immunostaining, 1.25×10^5 SH-SY5Y cells were transfected with 2 μg EGFP-SMN [16], EGFP-Gemin2, EGFP-Gemin3, EGFP-Gemin6 and EGFP-Gemin7 cDNA using the Amaxa-nucleofector device and reagents, specifying program G-004 as the optimized conditions to give high efficiency as recommended by the manufacturer. Immediately post-transfection cells were resuspended in 500 μl of RPMI supplemented with 10 μM *9-cis* retinoic acid (RA; Sigma–Aldrich R4643) and plated at a density of 1×10^4 cells/ml cultured onto glass coverslips. Cells were cultured for 72 h with the media replaced every 48 h. Cells were washed with PBS prior to fixation with 50% acetone/50% methanol. Fixed cells were incubated with anti-SMN monoclonal (MANSMA1; [17]) followed by incubation with a TRITC-conjugated anti-mouse IgG (Sigma) and DAPI.

2.5. Live cell imaging

SH-SY5Y cells were transfected with 2 μg EGFP-SMN [16], EGFP-Gemin2, EGFP-Gemin3, EGFP-Gemin6 and EGFP-Gemin7 cDNA using the Amaxa-nucleofector device and reagents according to manufacturers instructions and cultured on FluoroDishes™ (World Precision Instruments) in RPMI-1640 phenol red free media supplemented with 10% FCS and 10 μM retinoic acid for 72 h.

2.6. Microscopy

2.6.1. Fixed cell microscopy

Wide-field microscopy was performed using a Nikon TE 2000-U microscope with Hamamatsu camera as described elsewhere [16]. Images were acquired by taking Z-stacks and for Nikon TE 2000-U captured images, de-convolved using Openlab version 4.0.1 (Improvision). Images were processed using Photoshop 5.5 and CS3 (Adobe). Statistical analysis was performed using GraphPad Prism (version 5.01, GraphPad Software Inc.).

2.6.2. Live cell microscopy

Sealed dishes were transferred to a heated microscope stage and time lapse images acquired using Openlab version 4.0.1 (Improvision). Cells were imaged at exposure rates so that granules in distal regions were clearly visible (between 0.6 and 1 s depending upon magnification used) for a total of 60 s. Frame-by-frame measurements of GFP-construct movements were analysed using ImageJ (Rasband, W.S., ImageJ, U.S. National Institutes of Health, Bethesda, Maryland, USA, http://rsb.info.nih.gov/ij/, 1997–2005.)

3. Results

3.1. GFP-tagged Gemins are efficiently targeted to SMN neurite granules

SMN has previously been shown to form both stationary and dynamic granules in the axons of primary cells [4,5]. These granules are formed by both endogenous and transiently expressed

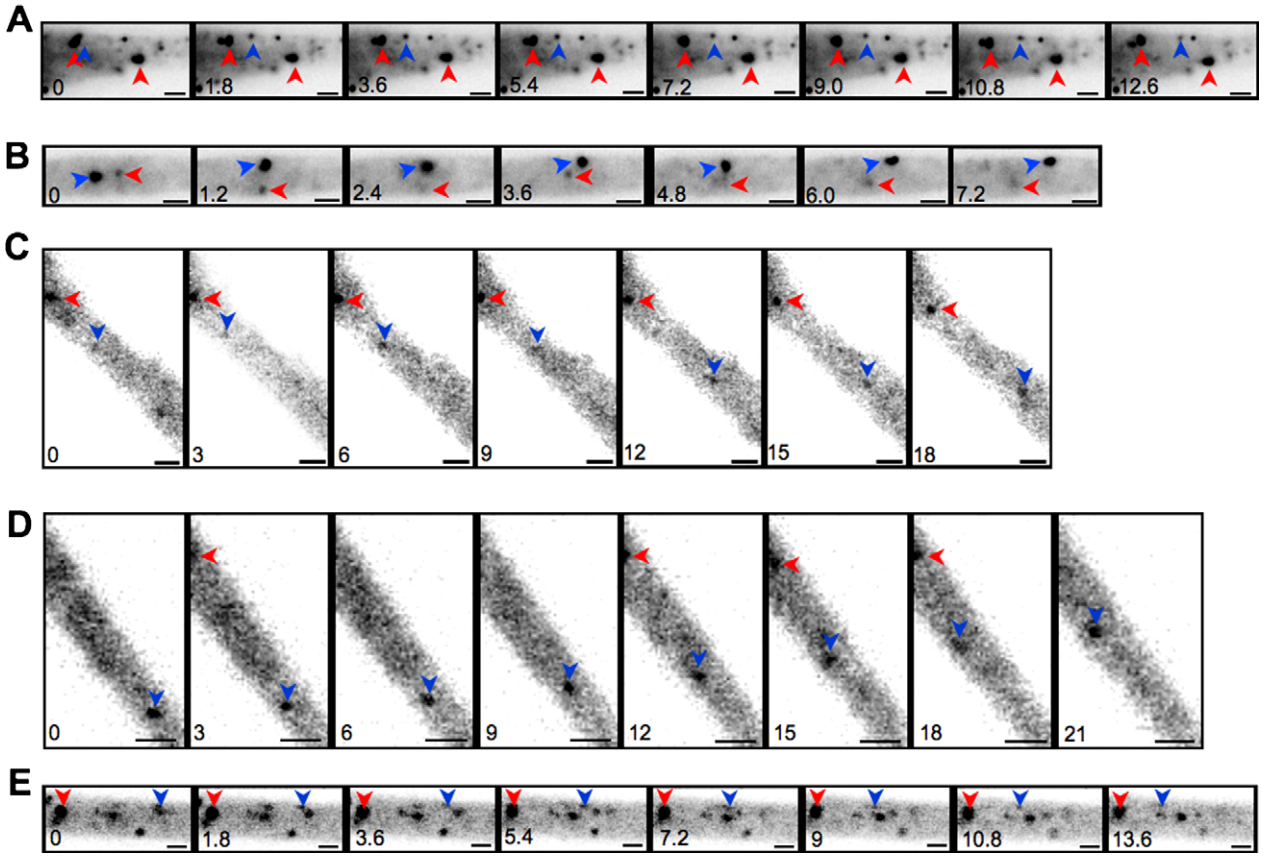

Fig. 2. SMN and Gemins are actively transported in small granules within neurites of SH-SY5Y cells. SH-SY5Y cells were transfected with GFP-tagged constructs and incubated for 72 h. Time-lapse imaging of neurites of transfected cells allowed the tracking of (A) GFP-SMN, (B) GFP-Gemin2, (C) GFP-Gemin3, (D) GFP-Gemin6 and (E) GFP-Gemin7. Small granules of each construct (red arrows), typically <0.5 μm diameter, showed signs of active transport (gross displacement >2 μm). Numerous larger granules (blue arrows), >0.5 μm diameter, showed no movement or oscillatory movements (blue arrows). The time of capture in seconds is indicated in each image. The scale bars represent 2 μm. (For interpretation of the references to colour in this figure legend, the reader is referred to the web version of this article.)

GFP-tagged SMN [4,5]. In addition, the SMN binding partners Gemin2 and Gemin3 have been identified in these granules in fixed cells [5], but only Gemin2 has been shown to co-migrate with SMN in the transport granules [5]. This leaves two very clear questions: (1) are the remaining Gemin proteins present in these granules; and (2) are the remaining Gemins targeted to both stationary and transport granules.

To determine if Gemin2, Gemin3, Gemin6 and Gemin7 are present in SMN-positive neurite granules, each Gemin was cloned into pEGFP vectors and over-expressed in differentiating SH-SY5Y cells.

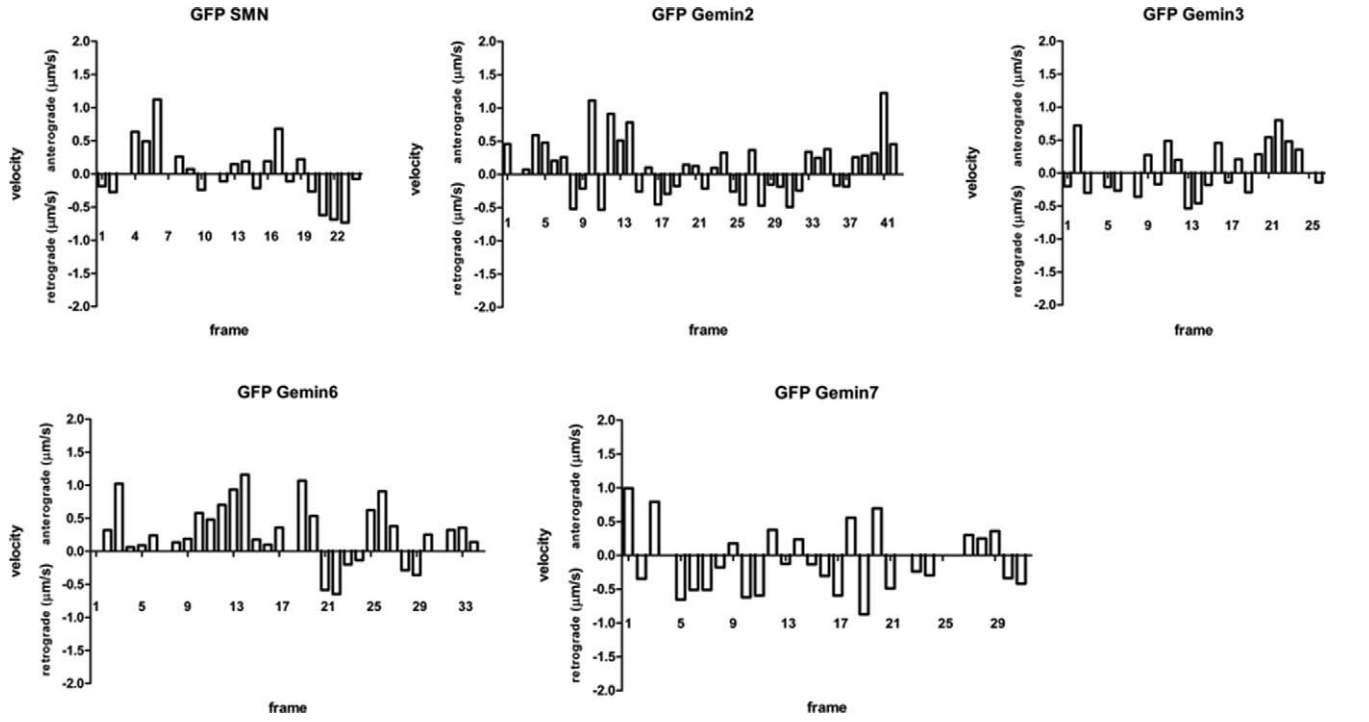

Fig. 3. Small GFP-SMN and GFP-Gemin granules exhibit similar rapid and bi-directional movements in neurites of SH-SY5Y cells. Histograms showing frame-by-frame analysis of granule velocities for each GFP-protein (GFP-SMN; GFP-Gemin3; GFP-Gemin6 and GFP-Gemin7), with each frame representing a second. Anterograde movements (μm/s) are positive and retrograde movements (μm/s) are negative.

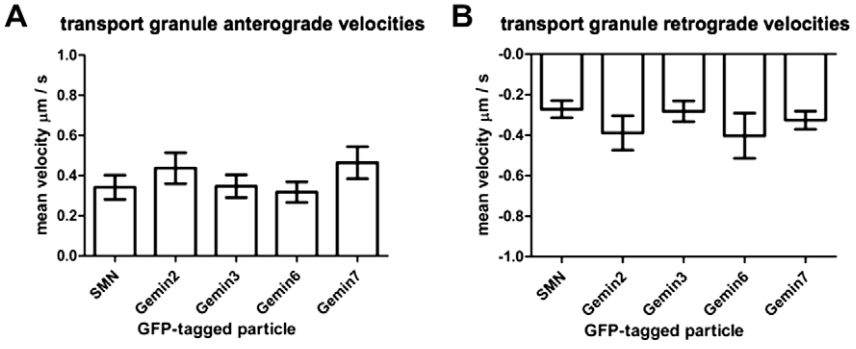

anterograde					
	SMN	Gemin2	Gemin3	Gemin6	Gemin7
Mean anterograde velocity (μm/s)	0.3417	0.4368	0.3471	0.3176	0.4646
Standard error of mean (SEM)	0.0604	0.07686	0.05674	0.05109	0.07965
Number (n)	10	10	10	8	8
retrograde					
	SMN	Gemin2	Gemin3	Gemin6	Gemin7
Mean retrograde velocity (μm/s)	-0.2727	-0.3895	-0.2829	-0.4034	-0.3267
Standard error of mean (SEM)	0.04216	0.08495	0.05123	0.1113	0.04434
Number (n)	10	8	10	8	10

Fig. 4. GFP-SMN and GFP-Gemin2, 3, 6, and 7 exhibit similar anterograde and retrograde velocities. All (A) anterograde and (B) retrograde velocities (μm/s) of each analysed GFP-particle were analysed for variance. Overall mean anterograde and retrograde velocities of GFP-tagged constructs were not significantly different ($p > 0.05$).

All four GFP-Gemin proteins were efficiently targeted to SMN granules in neurites (Fig. 1A–G), while control GFP-alone (GFPC1) was not (Fig. 1E). Using this approach we identified GFP-Gemin2 in 77.7% (±1.8 SEM) of SMN neurite granules; GFP-Gemin3 in 58.4% (±4.5 SEM); GFP-Gemin6 in 44.2% (±11.5 SEM) and GFP-Gemin7 in 46.1% (±4.5 SEM) (Fig. 1F and G). Transfection of GFPC1 was used to determine if the GFP-tag mediated targeting of each construct to SMN neurite granules. Given that GFPC1 is not efficiently targeted to SMN granules in neurites (Fig. 1E–G) it is unlikely that the GFP-tag is mediating the targeting to SMN neurite granules.

3.2. SMN and the Gemins are targeted to both stationary and actively transported neurite granules

SMN and Gemin2 have been shown to form both stationary and dynamic bodies [4,5]. Our initial analysis on fixed cells was unable to differentiate between SMN-stationary granules (SMN-SGs) and SMN-transport granules (SMN-TGs) in neurites of SH-SY5Y cells. Therefore, live cell imaging was performed on SH-SY5Y cells expressing the GFP-tagged Gemins to determine if each was present in both actively transported and stationary granules (Figs. 2–4). As with GFP-SMN, GFP-Gemin2, GFP-Gemin3, GFP-Gemin6 and GFP-Gemin7 were targeted to both stationary granules (SGs; Fig. 2, red arrows) and smaller transport granules (TGs; Fig. 2, blue arrows) that moved at velocities consistent with actively transported RNA granules (Figs. 2–4) [8,18]. Interestingly, SGs represented the clear majority of identified bodies for all GFP-constructs (Fig. 2; red arrows).

The identified TGs were similar in appearance to those previously reported for GFP-SMN, and GFP-Gemin2 [5] (Fig. 2, blue arrows; Figs. 3 and 4). This demonstrates two things: (1) that GFP-Gemin3, GFP-Gemin6 and GFP-Gemin7 are also present in actively transported granules (this is the first direct evidence that GFP-Gemin6 and GFP-Gemin7 are actively transported in neurites); and (2) that SH-SY5Y cells can be used as a functional working model to study intracellular transport in real time.

To further characterise TGs, the movement of 8–10 independent GFP-positive granules were analysed (Fig. 4). Selection criteria for the transport granules were defined as: (1) exhibiting directed movement (>2 μm in a single direction); and (2) visible within a field of view for a prolonged period of time (greater than 15 s). Recorded velocities of GFP-SMN and GFP-Gemin2 were consistent with previous reports [4,5], and the other GFP-Gemin proteins (Gemins 3, 6 and 7) exhibit similar dynamic bi-directional trajectory profiles (Figs. 3 and 4). For each construct the average mean velocities were calculated from the 8 to 10 analysed granules. For each, the net anterograde and retrograde movements and overall (gross) displacement are presented. All anterograde and retrograde velocities for each particle were analysed for statistically significant difference using a Kruskal–Wallis test with Dunns post-test. The mean anterograde and retrograde velocity of all combined GFP-particle movements are presented (Fig. 4). No statistical significance was found between the mean velocities for each GFP-construct (Fig. 4). Further statistical analysis of GFP-granules movements also failed to find any significant differences between their trajectories (Fig. 4). This data in combination with wide-field analysis of fixed cells (Fig. 1) suggests that SMN and Gemins are packaged into the same granules that are targeted to neurites. However, co-transfection studies need to be performed to confirm that this is the case.

4. Discussion

Here we report that the majority of the Gemin complex is targeted to the two subtypes of SMN-positive granules in neurites (Figs. 2–4). We have confirmed the presence of SMN and Gemin2 in these bodies, and for the first time demonstrated that Gemin3, Gemin6 and Gemin7 are also present (Figs. 2–4). This is important, because it shows that the Gemin complex appears to form a core complex that is present in the SMN neurite granules, suggesting the entire complex may be functionally involved in microtubule associated transport in neuronal cells [19].

In addition, we have analysed the velocities of granules formed by independent GFP-tagged Gemin proteins and confirmed that, like SMN, Gemin2 [4,5,7], Gemin3, Gemin6 and Gemin7 all form both larger stationary/oscillatory granules (SGs) and smaller actively transported granules (TGs) that move both rapidly and bi-directionally in neurites (Figs. 2–4). This is the first report of velocities of individual GFP-Gemin granules in neurites. Taken with the co-localisation data, this suggests that all the observed Gemin proteins co-localise (at least partially) with SMN in both stationary and transport granules. However, until co-transfection/live cell imaging is performed to confirm each co-migrates with SMN in the same bodies we cannot rule out the possibility that they form separate granules. For simplicity, during this discussion we refer to all SMN- and Gemin-positive neurite granules as SMN-Gemin neurite granules.

In keeping with previous reports, we demonstrate that SMN-Gemin granules in neurites exhibit characteristics of RNA transport granules forming both larger stationary granules [20], and smaller actively transporting granules [4,18,21]. Interestingly these SMN-Gemin neurite granules appear similar in size to SMN-positive nuclear bodies (Cajal bodies and their Gemini; [17,22]) and may share a similar function. Cajal bodies are believed to function as RNA and RNP processing sites [23,24]. They are involved in the sorting, maturation, and processing of newly formed U snRNPs [25–27]. SMN is known to play an integral role in the cytoplasmic assembly of the U snRNPs [28,29], as well as their subsequent nuclear import [30] and Cajal body targeting [31]. This demonstrates SMN is actively involved in the cellular targeting and transport of RNPs. Hypothetically, the predominant SMN-Gemin stationary granules could perform Cajal body-like functions, namely enabling the processing and sorting of transported cargoes, which are then moved along neurites in the dynamic SMN-Gemin transport granules.

Acknowledgments

This work was sponsored by the following agencies: (1) the Vandervell Foundation (P.J.Y. and R.M.); (2) IBCS / PMS (P.J.Y. and A.G.T.); (3) the SMA Trust (D.J.S. and P.J.Y.); and (4) the Northcott Medical Foundation (D.J.S. and P.J.Y.). The authors thank Prof. G.E. Morris for generously providing antibodies, and Dr. E.C. Young for proof reading and comments.

References

[1] L.M. Brzustowicz, C. Mérette, P.W. Kleyn, T. Lehner, L.H. Castilla, G.K. Penchaszadeh, K. Das, T.L. Munsat, J. Ott, T.C. Gilliam, Assessment of nonallelic genetic heterogeneity of chronic (type II and III) spinal muscular atrophy, Hum. Hered. 43 (1993) 380–387.
[2] S. Lefebvre, L. Burglen, S. Reboullet, O. Clermont, P. Burlet, L. Viollet, B. Benichou, C. Cruaud, P. Millasseau, M. Zeviani, Identification and characterization of a spinal muscular atrophy-determining gene, Cell 80 (1995) 155–165.
[3] B. Schrank, R. Götz, J.M. Gunnersen, J.M. Ure, K.V. Toyka, A.G. Smith, M. Sendtner, Inactivation of the survival motor neuron gene, a candidate gene for human spinal muscular atrophy, leads to massive cell death in early mouse embryos, Proc. Natl. Acad. Sci. USA 94 (1997) 9920–9925.
[4] H.L. Zhang, F. Pan, D. Hong, S.M. Shenoy, R.H. Singer, G.J. Bassell, Active transport of the survival motor neuron protein and the role of exon-7 in cytoplasmic localization, J. Neurosci. 23 (2003) 6627–6637.
[5] H. Zhang, L. Xing, W. Rossoll, H. Wichterle, R.H. Singer, G.J. Bassell, Multiprotein complexes of the survival of motor neuron protein SMN with

Gemins traffic to neuronal processes and growth cones of motor neurons, J. Neurosci. 26 (2006) 8622–8632.
[6] T.T. Le, L.T. Pham, M.E. Butchbach, H.L. Zhang, U.R. Monani, D.D. Coovert, T.O. Gavrilina, L. Xing, G.J. Bassell, A.H. Burghes, SMNDelta7, the major product of the centromeric survival motor neuron (SMN2) gene, extends survival in mice with spinal muscular atrophy and associates with full-length SMN, Hum. Mol. Genet. 14 (2005) 845–857.
[7] H. Zhang, L. Xing, R.H. Singer, G.J. Bassell, QNQKE targeting motif for the SMN–Gemin multiprotein complexin neurons, J. Neurosci. Res. 85 (2007) 2657–2667.
[8] M.A. Kiebler, G.J. Bassell, Neuronal RNA granules: movers and makers, Neuron 51 (2006) 685–690.
[9] S. Jablonka, K. Karle, B. Sandner, C. Andreassi, K. von Au, M. Sendtner, Distinct and overlapping alterations in motor and sensory neurons in a mouse model of spinal muscular atrophy, Hum. Mol. Genet. 15 (2006) 511–518.
[10] D.M. Tiruchinapalli, Y. Oleynikov, S. Kelic, S.M. Shenoy, A. Hartley, P.K. Stanton, R.H. Singer, G.J. Bassell, Activity-dependent trafficking and dynamic localization of zipcode binding protein 1 and beta-actin mRNA in dendrites and spines of hippocampal neurons, J. Neurosci. 23 (2003) 3251–3261.
[11] H.L. Zhang, T. Eom, Y. Oleynikov, S.M. Shenoy, D.A. Liebelt, J.B. Dictenberg, R.H. Singer, G.J. Bassell, Neurotrophin-induced transport of a beta-actin mRNP complex increases beta-actin levels and stimulates growth cone motility, Neuron 31 (2001) 261–275.
[12] F. Pan, S. Hüttelmaier, R.H. Singer, W. Gu, ZBP2 facilitates binding of ZBP1 to beta-actin mRNA during transcription, Mol. Cell. Biol. 27 (2007) 8340–8351.
[13] T. Eom, L.N. Antar, R.H. Singer, G.J. Bassell, Localization of a beta-actin messenger ribonucleoprotein complex with zipcode-binding protein modulates the density of dendritic filopodia and filopodial synapses, J. Neurosci. 23 (2003) 10433–10444.
[14] W. Rossoll, A.K. Kröning, U.M. Ohndorf, C. Steegborn, S. Jablonka, M. Sendtner, Specific interaction of Smn, the spinal muscular atrophy determining gene product, with hnRNP-R and gry-rbp/hnRNP-Q: a role for Smn in RNA processing in motor axons? Hum. Mol. Genet. 11 (2002) 93–105.
[15] A. Sharma, A. Lambrechts, l.e.T. Hao, T.T. Le, C.A. Sewry, C. Ampe, A.H. Burghes, G.E. Morris, A role for complexes of survival of motor neurons (SMN) protein with gemins and profilin in neurite-like cytoplasmic extensions of cultured nerve cells, Exp. Cell Res. 309 (2005) 185–197.
[16] R. Morse, D.J. Shaw, A.G. Todd, P.J. Young, Targeting of SMN to Cajal bodies is mediated by self-association, Hum. Mol. Genet. 16 (2007) 2349–2358.
[17] P.J. Young, T.T. Le, N. thi Man, A.H. Burghes, G.E. Morris, The relationship between SMN, the spinal muscular atrophy protein, and nuclear coiled bodies in differentiated tissues and cultured cells, Exp. Cell Res. 256 (2000) 365–374.
[18] M.S. Rook, M. Lu, K.S. Kosik, CaMKIIalpha 3' untranslated region-directed mRNA translocation in living neurons: visualization by GFP linkage, J. Neurosci. 20 (2000) 6385–6393.
[19] W. Rossoll, S. Jablonka, C. Andreassi, A.K. Kroning, K. Karle, U.R. Monani, M. Sendtner, Smn, the spinal muscular atrophy-determining gene product, modulates axon growth and localization of beta-actin mRNA in growth cones of motoneurons, J. Cell Biol. 163 (2003) 801–812.
[20] R.B. Knowles, J.H. Sabry, M.E. Martone, T.J. Deerinck, M.H. Ellisman, G.J. Bassell, K.S. Kosik, Translocation of RNA granules in living neurons, J. Neurosci. 16 (1996) 7812–7820.
[21] M. Kohrmann, M. Luo, C. Kaether, L. DesGroseillers, C.G. Dotti, M.A. Kiebler, Microtubule-dependent recruitment of Staufen-green fluorescent protein into large RNA-containing granules and subsequent dendritic transport in living hippocampal neurons, Mol. Biol. Cell 10 (1999) 2945–2953.
[22] P.J. Young, T.T. Le, M. Dunckley, T.M. Nguyen, A.H. Burghes, G.E. Morris, Nuclear gems and Cajal (coiled) bodies in fetal tissues: nucleolar distribution of the spinal muscular atrophy protein, SMN, Exp. Cell Res. 265 (2001) 252–261.
[23] D. Stanek, K.M. Neugebauer, The Cajal body: a meeting place for spliceosomal snRNPs in the nuclear maze, Chromosoma 115 (2006) 343–354.
[24] D. Stanek, J. Pridalová-Hnilicová, I. Novotny, M. Huranová, M. Blazíková, X. Wen, A.K. Sapra, K.M. Neugebauer, Spliceosomal small nuclear ribonucleoprotein particles repeatedly cycle through Cajal bodies, Mol. Biol. Cell 19 (2008) 2534–2543.
[25] J.E. Sleeman, P. Ajuh, A.I. Lamond, SnRNP protein expression enhances the formation of Cajal bodies containing p80-coilin and SMN, J. Cell Sci. 114 (2001) 4407–4419.
[26] S.C. Ogg, A.I. Lamond, Cajal bodies and coilin–moving towards function, J. Cell Biol. 159 (2002) 17–21.
[27] B.E. Jády, X. Darzacq, K.E. Tucker, A.G. Matera, E. Bertrand, T. Kiss, Modification of Sm small nuclear RNAs occurs in the nucleoplasmic Cajal body following import from the cytoplasm, EMBO J. 22 (2003) 1878–1888.
[28] J. Yong, T.J. Golembe, D.J. Battle, L. Pellizzoni, G. Dreyfuss, SnRNAs contain specific SMN-binding domains that are essential for snRNP assembly, Mol. Cell. Biol. 24 (2004) 2747–2756.
[29] L. Wan, D.J. Battle, J. Yong, A.K. Gubitz, S.J. Kolb, J. Wang, G. Dreyfuss, The survival of motor neurons protein determines the capacity for snRNP assembly: biochemical deficiency in spinal muscular atrophy, Mol. Cell. Biol. 25 (2005) 5543–5551.
[30] U. Narayanan, J.K. Ospina, M.R. Frey, M.D. Hebert, A.G. Matera, SMN, the spinal muscular atrophy protein, forms a pre-import snRNP complex with snurportin1 and importin beta, Hum. Mol. Genet. 11 (2002) 1785–1795.
[31] A.G. Matera, M.D. Hebert, The survival motor neurons protein uses its ZPR for nuclear localization, Nat. Cell Biol. 3 (2001) E93–E95.